

1 **SARS-CoV-2 Encodes a PPxY Late Domain Motif Known to Enhance Budding and**
2 **Spread in Enveloped RNA Viruses**

3

4 Halim Maaroufi

5 Institut de biologie intégrative et des systèmes (IBIS), Université Laval, Quebec City,

6 Canada

7 Halim.maaroufi@ibis.ulaval.ca

8

9 **ABSTRACT**

10 The current COVID-19 (Coronavirus Disease-2019) pandemic is affecting the health
11 and/or socioeconomic welfare of almost everyone in the world. Finding vaccines and
12 therapeutics is therefore urgent, but elucidation of the molecular mechanisms that allow
13 some viruses to cross host species boundaries, becoming a threat to human health, must
14 also be given close attention. Here, analysis of all proteins of SARS-CoV-2 revealed a
15 unique PPxY Late (L) domain motif, ²⁵PPAY²⁸, in a spike (S) protein inside a predicted
16 hot disordered loop subject to phosphorylation and binding. PPxY motifs in enveloped
17 RNA viruses are known to recruit Nedd4 E3 ubiquitin ligases and ultimately the ESCRT
18 complex to enhance virus budding and release, resulting in higher viral loads, hence
19 facilitating new infections. Interestingly, proteins of SARS-CoV-1 do not feature PPxY
20 motifs, which could explain why SARS-CoV-2 is more contagious than SARS-CoV-1.
21 Should an experimental assessment of this hypothesis show that the PPxY motif plays the
22 same role in SARS-CoV-2 as it does in other enveloped RNA viruses, this motif will
23 become a promising target for the development of novel host-oriented antiviral therapeutics
24 for preventing S proteins from recruiting Nedd4 E3 ubiquitin ligase partners.

25

26 **KEYWORDS** SARS-CoV-2; Spike protein; PPxY Late Domain Motif; WW-domain;
27 Nedd4 E3 ubiquitin ligases; Budding; Spread

28 INTRODUCTION

29

30 The current COVID-19 (Coronavirus Disease-2019) pandemic caused by SARS-CoV-2
31 from Wuhan is affecting the health (both physical and psychological) and/or
32 socioeconomic welfare of almost everyone in the world. Finding vaccines and therapeutics
33 to fight SARS-CoV-2 is therefore urgent. In addition, it is imperative, now and in the
34 future, to maintain research efforts aimed at elucidating the molecular mechanisms
35 (tropism, cell entry, multiplication and spread, etc.) used by emerging viruses such as
36 SARS-CoV-2 to infect humans. An improved understanding of these mechanisms should
37 be viewed as an investment in our future to prevent and/or control the emergence of
38 dangerous viruses that could have as or more severe consequences for humanity than
39 SARS-CoV-2. The family *Coronaviridae* (CoVs) is large and comprises enveloped,
40 positive-sense, single-stranded RNA viruses (Graham and Baric, 2010; Li, 2013). Among
41 all RNA viruses, CoVs possess the largest genomes, ranging in size between 27 and 32 kb.
42 The subfamily *Coronavirinae* comprises four genera, *Alpha-*, *Beta-*, *Delta-* and
43 *Gammacoronavirus*, which can infect both mammalian and avian species.
44 Phylogenetically, SARS-CoV-2 is more closely related to SARS-CoV-1 than to MERS-
45 CoV, but all three are betacoronaviruses (betaCoVs) (de Wit et al., 2016).

46

47 The envelope-anchored SARS-CoV-2 spike (S) is a multifunctional glycoprotein with
48 1273 amino acid residues. Its structure was solved as a homotrimeric molecule with several
49 domains. The S protein is subdivided into S1 and S2 subunits. S1 is formed by two
50 domains, an N-terminal domain (NTD) and a C-terminal receptor-binding domain (RBD)
51 that binds specifically to the host receptor angiotensin-converting enzyme 2 (ACE2) on the
52 host cell surface (Li, 2012). The S2 subunit, which is also multidomain, induces viral-host
53 membrane fusion.

54

55 The viral proline-rich Pro-Pro-x-Tyr (PPxY) Late or L-domain motif (Chen and Sudol,
56 1995) interacts with host proteins containing the WW-domain. The term “Late” reflects a
57 late function in the virus life cycle (Garnier et al., 1996; Freed, 2002). L-domain motifs are
58 identified in enveloped RNA viruses such as in the Gag protein of a number of retroviruses

59 and in the matrix of arenaviruses, rhabdoviruses and filoviruses (Baillet et al., 2019;
60 Bieniasz, 2006; Wirblich et al., 2008). The WW-domain is a small domain of 35–40 amino
61 acids, named after two conserved tryptophan (W) residues in the sequence (Bork and Sudol,
62 1994). It is a fold of three-stranded antiparallel β -sheets that contains two ligand-binding
63 grooves (Huang et al., 2000; Kanelis et al., 2001). RNA viruses use PPxY L-domain motifs
64 to recruit specific WW-domain of host proteins of either Nedd4 (Neuronal precursor cell-
65 Expressed Developmentally Down-regulated 4), or Nedd4 family members to facilitate
66 their egress and spread (Bieniasz, 2006). Nedd4 family proteins have three domains, N-
67 terminal lipid binding (C2) domain; WW modules, present in multiple copies; and a C-
68 terminal Hect (for homologous to E6-associated protein C terminus) domain that contains
69 the ubiquitin ligase activity.

70

71 Previous and current investigations are focusing on understanding the first step that allows
72 SARS-CoV-1 and SARS-CoV-2 to enter host cells. This research examines primarily the
73 interaction between the C-terminal receptor-binding domain (RBD) of S proteins and the
74 host receptor angiotensin-converting enzyme 2 (ACE2). Here, the molecular mechanism
75 of the last step (late function virus life cycle) of budding and release of virus is presented.
76 The N-terminal of SARS-CoV-2 spike protein contains a PPxY L-domain motif that is
77 known to hijack host WW-domain of Nedd4 E3 ubiquitin ligases and ultimately the
78 ESCRT (Endosomal Sorting Complex Required for Transport) complex to enhance virus
79 budding and spread. Importantly, this motif is absent in SARS-CoV-1, which could explain
80 why SARS-CoV-2 is more contagious than SARS-CoV-1. Development of a novel host-
81 oriented inhibitor targeting molecular interactions between PPxY and the host WW-
82 domain holds potential in the fight against SARS-CoV-2 infection.

83 **RESULTS AND DISCUSSION**

84

85 *The N-terminal of S protein contains a PPxY L-domain motif*

86

87 Sequence analysis of SARS-CoV-2 spike protein using the Eukaryotic Linear Motif (ELM)
88 resource (<http://elm.eu.org/>) revealed a short linear motif (SLiMs) known as PPxY Late
89 (L-) domain motif, ²⁵PPAY²⁸ in the N-terminus of the S1 subunit. The PPxY L-domain
90 motif is known to interact with proteins containing WW-domain(s). L-domain motifs have
91 been identified in single-stranded enveloped RNA viruses (Table 1), including in the Gag
92 proteins of several retroviruses and in the matrix of arenaviruses, rhabdoviruses and
93 filoviruses (Baillet et al., 2019; Bieniasz, 2006; Wirblich et al., 2008). RNA viruses use
94 PPxY L-domain motifs to recruit specific WW-domains of host Nedd4 family members
95 and ultimately the ESCRT complex to facilitate their budding and egress (Bieniasz, 2006).
96 Interestingly, the SARS-CoV-2 S protein and Nedd4 can be S-palmitoylated, suggesting
97 that they can localize to similar membrane subdomains (Petit et al., 2007; Gordon et al.,
98 2020; Chesarino et al., 2014) and may therefore be able to interact. The ScanProsite tool
99 (<https://prosite.expasy.org/scanprosite/>) showed that the PPxY motif is present in SARS-
100 CoV-2 but absent from SARS-CoV-1 proteins. It has been reported in enveloped RNA
101 viruses that PPxY motif recruits Nedd4 E3 ubiquitin ligases and ultimately the ESCRT
102 complex to enhance virus budding and release that means a high viral load, thus facilitating
103 new infections. This suggests in SARS-CoV-2 that the PPxY motif, through its role in
104 enhancing the viral load, could play a role in making SARS-CoV-2 more contagious than
105 SARS-CoV-1 (To et al., 2020).

106

107 The PPxY motif is also present in the S protein of bat RaTG13 and pangolin GX-P5L, two
108 SARS-related coronaviruses (Fig. 1A). Moreover, S proteins with PPxY motif are
109 phylogenetically close (Fig. 1C). Interestingly, alignment of S protein sequences of two
110 pangolin coronaviruses showed only two differences in the S1 subunit (amino acid at
111 position 25 (P/Q) and deletion of ⁴⁴⁸GY⁴⁴⁹ in pangolin GX-P1E) (Lam et al., 2020; Zhang
112 et al., 2020). In the future, it would be interesting to compare virulence of pangolin GX-
113 P1E and pangolin GX-P5L coronaviruses to know if the loss of PPxY motif is important
114 for virulence. Figure 1B shows differences among coronaviruses in nucleotide composition

115 for the codon corresponding to Pro25 in SARS-CoV-2. Transition mutations (purine (A,
116 G) to purine or pyrimidine (C, T) to pyrimidine mutations) are more likely than
117 transversion (purine to pyrimidine or vice versa) mutations. Additionally, most
118 substitutions occur in the third nucleotide of codons (silent mutations), less frequently in
119 the first nucleotide, and the least frequently in the second nucleotide (Wang et al., 2007).
120 Therefore, a mutation from Ala (GCT) to Pro (CCT) is more likely to occur than one from
121 Gln (CAG) to Pro (CCG). Moreover, a double mutation Asn (AAT) to Proline (CCT) is
122 even less probable (Fig. 1B).

123

124 *PPxY L-domain motif is in hot region*

125

126 Scanning the SARS-CoV-2 S protein sequence with the DisEMBL software (Linding et
127 al., 2003) revealed, in the N-terminal region, a unique hot disordered loop
128 ¹⁹TTRTQLPPAYTNSFT³³ that includes the PPxY motif (Table 2), and this loop contains
129 additional motifs. Indeed, the PPxY motif shares its tyrosine with an overlapping
130 ²⁸YTNSF³² motif (Fig. 1A) that enables binding to the SH2 domain of STAP1 when its
131 Tyr28 is phosphorylated. STAP1 (Signal Adaptor Protein 1) is an adaptor protein with an
132 SH2 and a PH class of lipid-binding domain (Wang et al., 1994). It is expressed in
133 lymphoid cells and is phosphorylated by the Tec tyrosine kinase (Tec TK), which
134 participates in B cell antigen receptor signaling (Ohya et al., 1999; Yang et al., 2001). The
135 middle T-antigen of the polyoma virus, with its tyrosine residue in a phosphorylated state,
136 has been shown to act as a binding site for the SH2 domain of the phosphatidylinositol-
137 3'OH kinase 85K subunit (Dilworth et al. 1994). Another site, ²⁸YTNS³¹ in the S protein,
138 is also Tyr-phosphorylation-dependent for binding SH2 domain (Lin et al., 2006).

139

140 The hot region of the S protein also contains a Ser/Thr phosphorylated motif. Indeed, the
141 PPxY motif shares its Pro25 with an overlapping ¹⁹TTRTQLP²⁵ motif that could be
142 phosphorylated at TQ by a phosphatidylinositol 3- and/or 4-kinase (PIKKs). The Gln (Q)
143 beside to the target Ser/Thr is critical for substrate recognition. PIKKs are atypical Ser/Thr
144 kinases found only in eukaryotes (Imseng et al., 2108; Angira et al., 2020). Interestingly,
145 Yang et al. (2012) showed that phosphatidylinositol 4-kinase III β (PI4KB) is required for
146 cellular entry by pseudoviruses bearing the SARS-CoV-1 S protein. This cell entry is

147 highly inhibited by knockdown of PI4KB. Moreover, the same authors showed that PI4KB
148 does not affect virus entry at the SARS-CoV-1 S-ACE2 interface. Finally, the motif
149 ²⁶PAYTNSF³³ is recognised by the Ser/Thr kinase GSK3 (Glycogen synthase kinase 3).
150 Interestingly, the lipid kinase phosphatidylinositol 4-kinase II α (PI4KII α) was reported to
151 be a substrate of GSK3 (Robinson et al. 2014). This finding establishes a link with
152 ¹⁹TTRTQLP²⁵ motif, described above, that is predicted to be phosphorylated by GSK3.
153 In summary, proteins that interact with this hot disordered loop are connected to lipids
154 (membrane), particularly with phosphatidylinositol, and bindings is regulated by
155 phosphorylation. Recently, Besson et al. (2019) showed that the mitogen-activated
156 protein kinase pathway and phosphatidylinositol metabolism are involved in the later
157 stage of RABV infection.

158

159 *Interactions of PPxY L-domain motif with Nedd4-WW3-domain Ub ligase*

160

161 To compare the interaction between the PPAY S protein and the Nedd4WW-domain with
162 those of other PPxY-Nedd4WW-domain complexes, molecular docking was performed
163 using the software AutoDock vina (Trott and Olson, 2010). Fig. 2 shows that the
164 ²³QLPPAYTNS³¹ peptide of SARS-CoV-2 S protein is localized in the same region as
165 ¹¹²TAPPEYMEA¹²⁰ motif of the Zaire Ebola virus Matrix protein VP40 (PDBid: 2KQ0),
166 and important amino acid residues of the SARS-CoV-2 peptide are superposed with
167 corresponding residues of the Ebola VP40 peptide, with the exception of different
168 orientations for the aromatic ring of tyrosine (Fig. 2B and C). Iglesias-Bexiga et al. (2019)
169 reported that the Nedd4-WW3 binding site is highly plastic and can accommodate PPxY-
170 containing ligands with varying orientations. This structural superposition with PPxY of
171 VP40 confirms the reliability of the AutoDock vina peptide docking module. Detailed
172 knowledge of the molecular interaction between the ²³QLPPAYTNS³¹ motif and the
173 Nedd4WW-domain will help design a peptide able to mimic the surface of the Nedd4 WW-
174 domain and strongly bind the ²³QLPPAYTNS³¹ peptide, thus preventing the recruitment
175 of Nedd4 E3 ubiquitin ligase by the SARS-CoV-2 S protein (Zaidman and Wolfson, 2016).
176 Indeed, Han et al. (2014) have developed two lead compounds that specifically block the
177 VP40 PPxY-host Nedd4 interaction, displaying anti-budding activity in the nanomolar
178 range.

179 **MATERIALS AND METHODS**

180

181 *Sequence analysis*

182

183 To search probable short linear motifs (SLiMs), SARS-CoV-2 spike protein sequence was
184 scanned using the eukaryotic linear motif (ELM) resource (<http://elm.eu.org/>). The PPxY
185 L-domain motif was searched in proteins of SARS-CoV-2 and SARS-CoV-1 using
186 <https://prosite.expasy.org/scanprosite/>

187

188 *3D modeling and molecular docking*

189

190 Unfortunately, the region containing the ²³QLPPAYTNS³¹peptide has not been resolved
191 in any known structure of spike S protein. Therefore, the Pep-Fold (Thevenet et al., 2012)
192 software was used to generate a *de novo* model of this peptide. Model quality of the peptide
193 was assessed by analysis of a Ramachandran plot through PROCHECK (Vaguine et al.,
194 1999).

195

196 Docking of the peptide into the human Nedd4 3rd WW-domain (PDBid: 2KQ0_A) was
197 performed using the software AutoDock vina (Trott and Olson, 2010). The 3D complex
198 containing the human Nedd4 3rd WW-domain and the peptide was refined using
199 FlexPepDock (London et al., 2011), which allows full flexibility to the peptide and side-
200 chain flexibility to the receptor.

201

202 *Phylogeny*

203

204 Amino acid sequences of different spike (S) proteins, namely those of SARS-CoV-2
205 (accession: YP_009724390.1), SARS-CoV-1 (P59594.1), bat_coronavirus_RaTG13
206 (QHR63300.2), pangolin_PCoV_GX-P5L (QIA48632.1), pangolin_PCoV_GX-P1E
207 (QIA48623.1), bat_CoVZC45_CoV (AVP78031.1) and bat_Rs4874_CoV (ATO98205.1),
208 were aligned using the T-coffee software (Rius et al., 2011). This multiple alignment was
209 then used to estimate the phylogenetic relationships between SARS-CoV-2 and others
210 coronaviruses. The phylogenetic tree was constructed using MrBayes (Huelsenbeck and
211 Ronquist, 2001) with the following parameters: Likelihood model (Number of substitution

212 types: 6(GTR); Substitution model: Poisson; Rates variation across sites: Invariable +
213 gamma); Markov Chain Monte Carlo parameters (number of generations: 100 000; Sample
214 a tree every: 1000 generations) and Discard first 500 trees sampled (burnin).

215

216 **ACKNOWLEDGMENTS**

217 I would like to thank the IBIS bioinformatics group for their assistance. I am grateful to
218 Dr. Michel Cusson, Université Laval, for the revision of the manuscript.

219

220 **CONFLICT OF INTERESTED**

221 The author declares that he has no conflicts of interest.

222

223 **REFERENCES**

224

225 Angira, D., Shaik, A., Thiruvencatam, V., 2020. Structural and strategic landscape of
226 PIKK protein family and their inhibitors: an overview. *Front. Biosci.* 25, 1538–1567.

227

228 Baillet, N., Krieger, S., Carnec, X., Mateo, M., Journeaux, A., Merabet, O., Caro, V.,
229 Tangy, F., Vidalain, P.-O., Baize, S., 2019. E3 Ligase ITCH Interacts with the Z Matrix
230 Protein of Lassa and Mopeia Viruses and Is Required for the Release of Infectious
231 Particles. *Viruses* 12. <https://doi.org/10.3390/v12010049>

232

233 Besson, B., Kim, S., Kim, T., Ko, Y., Lee, S., Larrous, F., Song, J., Shum, D., Grailhe,
234 R., Bourhy, H., 2019. Kinome-Wide RNA Interference Screening Identifies Mitogen-
235 Activated Protein Kinases and Phosphatidylinositol Metabolism as Key Factors for
236 Rabies Virus Infection. *mSphere* 4. <https://doi.org/10.1128/mSphere.00047-19>

237

238 Bieniasz, P.D., 2006. Late budding domains and host proteins in enveloped virus release.
239 *Virology* 344, 55–63. <https://doi.org/10.1016/j.virol.2005.09.044>

240

241 Bork, P., Sudol, M., 1994. The WW domain: a signalling site in dystrophin? *Trends*
242 *Biochem. Sci.* 19, 531–533. [https://doi.org/10.1016/0968-0004\(94\)90053-1](https://doi.org/10.1016/0968-0004(94)90053-1)

243

244 Bouamr, F., Melillo, J.A., Wang, M.Q., Nagashima, K., de Los Santos, M., Rein, A.,
245 Goff, S.P., 2003. PPPYVEPTAP motif is the late domain of human T-cell leukemia virus

- 246 type 1 Gag and mediates its functional interaction with cellular proteins Nedd4 and
247 Tsg101 [corrected]. *J. Virol.* 77, 11882–11895. [https://doi.org/10.1128/jvi.77.22.11882-](https://doi.org/10.1128/jvi.77.22.11882-11895.2003)
248 [11895.2003](https://doi.org/10.1128/jvi.77.22.11882-11895.2003)
- 249
250 Chen, H.I., Sudol, M., 1995. The WW domain of Yes-associated protein binds a proline-
251 rich ligand that differs from the consensus established for Src homology 3-binding
252 modules. *Proc. Natl. Acad. Sci. U. S. A.* 92, 7819–7823.
253 <https://doi.org/10.1073/pnas.92.17.7819>
- 254
255 Chesarino, N.M., Hach, J.C., Chen, J.L., Zaro, B.W., Rajaram, M.V., Turner, J.,
256 Schlesinger, L.S., Pratt, M.R., Hang, H.C., Yount, J.S., 2014. Chemoproteomics reveals
257 Toll-like receptor fatty acylation. *BMC Biol.* 12, 91. [https://doi.org/10.1186/s12915-014-](https://doi.org/10.1186/s12915-014-0091-3)
258 [0091-3](https://doi.org/10.1186/s12915-014-0091-3)
- 259
260 de Wit, E., van Doremalen, N., Falzarano, D., Munster, V.J., 2016. SARS and MERS:
261 recent insights into emerging coronaviruses. *Nat. Rev. Microbiol.* 14, 523–534.
262 <https://doi.org/10.1038/nrmicro.2016.81>
- 263
264 Dilworth, S.M., Brewster, C.E., Jones, M.D., Lanfrancone, L., Pelicci, G., Pelicci, P.G.,
265 1994. Transformation by polyoma virus middle T-antigen involves the binding and
266 tyrosine phosphorylation of Shc. *Nature* 367, 87–90. <https://doi.org/10.1038/367087a0>
- 267
268 Dolnik, O., Kolesnikova, L., Stevermann, L., Becker, S., 2010. Tsg101 is recruited by a
269 late domain of the nucleocapsid protein to support budding of Marburg virus-like
270 particles. *J. Virol.* 84, 7847–7856. <https://doi.org/10.1128/JVI.00476-10>
- 271
272 Freed, E.O., 2002. Viral late domains. *J. Virol.* 76, 4679–4687.
273 <https://doi.org/10.1128/jvi.76.10.4679-4687.2002>
- 274
275 Garnier, L., J. W. Wills, M. F. Verderame and M. Sudol (1996). "WW domains and
276 retrovirus budding." *Nature* 381(6585): 744-745. <https://doi.org/10.1038/381744a0>
- 277
278 Graham, R.L., Baric, R.S., 2010. Recombination, reservoirs, and the modular spike:
279 mechanisms of coronavirus cross-species transmission. *J. Virol.* 84, 3134–3146.
280 <https://doi.org/10.1128/JVI.01394-09>
- 281
282 Gordon, D.E., Jang, G.M., Bouhaddou, M., Xu, J., Obernier, K., O’Meara, M.J., Guo,

283 J.Z., Swaney, D.L., Tummino, T.A., Huettenhain, R., Kaake, R.M., Richards, A.L.,
284 Tutuncuoglu, B., Foussard, H., Batra, J., Haas, K., Modak, M., Kim, M., Haas, P.,
285 Polacco, B.J., Braberg, H., Fabius, J.M., Eckhardt, M., Soucheray, M., Bennett, M.J.,
286 Cakir, M., McGregor, M.J., Li, Q., Naing, Z.Z.C., Zhou, Y., Peng, S., Kirby, I.T.,
287 Melnyk, J.E., Chorba, J.S., Lou, K., Dai, S.A., Shen, W., Shi, Y., Zhang, Z., Barrio-
288 Hernandez, I., Memon, D., Hernandez-Armenta, C., Mathy, C.J.P., Perica, T., Pilla, K.B.,
289 Ganesan, S.J., Saltzberg, D.J., Ramachandran, R., Liu, X., Rosenthal, S.B., Calviello, L.,
290 Venkataramanan, S., Liboy-Lugo, J., Lin, Y., Wankowicz, S.A., Bohn, M., Sharp, P.P.,
291 Trenker, R., Young, J.M., Caverio, D.A., Hiatt, J., Roth, T.L., Rathore, U., Subramanian,
292 A., Noack, J., Hubert, M., Roesch, F., Vallet, T., Meyer, B., White, K.M., Miorin, L.,
293 Rosenberg, O.S., Verba, K.A., Agard, D., Ott, M., Emerman, M., Ruggero, D., García-
294 Sastre, A., Jura, N., von Zastrow, M., Taunton, J., Ashworth, A., Schwartz, O., Vignuzzi,
295 M., d'Enfert, C., Mukherjee, S., Jacobson, M., Malik, H.S., Fujimori, D.G., Ideker, T.,
296 Craik, C.S., Floor, S., Fraser, J.S., Gross, J., Sali, A., Kortemme, T., Beltrao, P., Shokat,
297 K., Shoichet, B.K., Krogan, N.J., 2020. A SARS-CoV-2-Human Protein-Protein
298 Interaction Map Reveals Drug Targets and Potential Drug-Repurposing. bioRxiv.
299 <https://doi.org/10.1101/2020.03.22.002386>

300

301 Han, Z., Lu, J., Liu, Y., Davis, B., Lee, M.S., Olson, M.A., Ruthel, G., Freedman, B.D.,
302 Schnell, M.J., Wrobel, J.E., Reitz, A.B., Harty, R.N., 2014. Small-molecule probes
303 targeting the viral PPxY-host Nedd4 interface block egress of a broad range of RNA
304 viruses. *J. Virol.* 88, 7294–7306. <https://doi.org/10.1128/JVI.00591-14>

305

306 Harty, R.N., Brown, M.E., McGettigan, J.P., Wang, G., Jayakar, H.R., Huibregtse, J.M.,
307 Whitt, M.A., Schnell, M.J., 2001. Rhabdoviruses and the cellular ubiquitin-proteasome
308 system: a budding interaction. *J. Virol.* 75, 10623–10629.
309 <https://doi.org/10.1128/JVI.75.22.10623-10629.2001>

310

311 Harty, R.N., Brown, M.E., Wang, G., Huibregtse, J., Hayes, F.P., 2000. A PPxY motif
312 within the VP40 protein of Ebola virus interacts physically and functionally with a
313 ubiquitin ligase: implications for filovirus budding. *Proc. Natl. Acad. Sci. U. S. A.* 97,
314 13871–13876. <https://doi.org/10.1073/pnas.250277297>

315

316 Huang, X., Poy, F., Zhang, R., Joachimiak, A., Sudol, M., Eck, M.J., 2000. Structure of a
317 WW domain containing fragment of dystrophin in complex with beta-dystroglycan. *Nat.*
318 *Struct. Biol.* 7, 634–638. <https://doi.org/10.1038/77923>

319

320 Huelsenbeck, J.P., Ronquist, F., 2001. MRBAYES: Bayesian inference of phylogenetic
321 trees. *Bioinformatics* 17, 754–755. <https://doi.org/10.1093/bioinformatics/17.8.754>

322

323 Iglesias-Bexiga, M., Palencia, A., Corbi-Verge, C., Martin-Malpartida, P., Blanco, F.J.,
324 Macias, M.J., Cobos, E.S., Luque, I., 2019. Binding site plasticity in viral PPxY Late
325 domain recognition by the third WW domain of human NEDD4. *Sci. Rep.* 9, 15076.
326 <https://doi.org/10.1038/s41598-019-50701-3>

327

328 Imseng, S., Aylett, C.H., Maier, T., 2018. Architecture and activation of
329 phosphatidylinositol 3-kinase related kinases. *Curr. Opin. Struct. Biol.* 49, 177–189.
330 <https://doi.org/10.1016/j.sbi.2018.03.010>

331

332 Kanelis, V., Rotin, D., Forman-Kay, J.D., 2001. Solution structure of a Nedd4 WW
333 domain-ENaC peptide complex. *Nat. Struct. Biol.* 8, 407–412.
334 <https://doi.org/10.1038/87562>

335

336 Lam, T.T.-Y., Shum, M.H.-H., Zhu, H.-C., Tong, Y.-G., Ni, X.-B., Liao, Y.-S., Wei, W.,
337 Cheung, W.Y.-M., Li, W.-J., Li, L.-F., Leung, G.M., Holmes, E.C., Hu, Y.-L., Guan, Y.,
338 2020. Identifying SARS-CoV-2 related coronaviruses in Malayan pangolins. *Nature*.
339 <https://doi.org/10.1038/s41586-020-2169-0>

340

341 Li, F., 2013. Receptor recognition and cross-species infections of SARS coronavirus.
342 *Antiviral Res.* 100, 246–254. <https://doi.org/10.1016/j.antiviral.2013.08.014>

343

344 Li, F., 2012. Evidence for a common evolutionary origin of coronavirus spike protein
345 receptor-binding subunits. *J. Virol.* 86, 2856–2858. <https://doi.org/10.1128/JVI.06882-11>

346

347 Lin, W., Kim, S.S., Yeung, E., Kamegaya, Y., Blackard, J.T., Kim, K.A., Holtzman,
348 M.J., Chung, R.T., 2006. Hepatitis C virus core protein blocks interferon signaling by
349 interaction with the STAT1 SH2 domain. *J. Virol.* 80, 9226–9235.
350 <https://doi.org/10.1128/JVI.00459-06>

351

352 Linding, R., Jensen, L.J., Diella, F., Bork, P., Gibson, T.J., Russell, R.B., 2003. Protein
353 disorder prediction: implications for structural proteomics. *Structure* 11, 1453–1459.
354 <https://doi.org/10.1016/j.str.2003.10.002>

355

356 London, N., Raveh, B., Cohen, E., Fathi, G., Schueler-Furman, O., 2011. Rosetta
357 FlexPepDock web server--high resolution modeling of peptide-protein interactions.
358 *Nucleic Acids Res.* 39, W249–53. <https://doi.org/10.1093/nar/gkr431>

359

360 Ohya, K., Kajigaya, S., Kitanaka, A., Yoshida, K., Miyazato, A., Yamashita, Y.,
361 Yamanaka, T., Ikeda, U., Shimada, K., Ozawa, K., Mano, H., 1999. Molecular cloning of
362 a docking protein, BRDG1, that acts downstream of the Tec tyrosine kinase. *Proc. Natl.*
363 *Acad. Sci. U. S. A.* 96, 11976–11981. <https://doi.org/10.1073/pnas.96.21.11976>

364

365 Petit, C.M., Chouljenko, V.N., Iyer, A., Colgrove, R., Farzan, M., Knipe, D.M.,
366 Kousoulas, K.G., 2007. Palmitoylation of the cysteine-rich endodomain of the SARS-
367 coronavirus spike glycoprotein is important for spike-mediated cell fusion. *Virology* 360,
368 264–274. <https://doi.org/10.1016/j.virol.2006.10.034>

369

370 Rius, J., Cores, F., Solsona, F., van Hemert, J.I., Koetsier, J., Notredame, C., 2011. A
371 user-friendly web portal for T-Coffee on supercomputers. *BMC Bioinformatics* 12, 150.
372 <https://doi.org/10.1186/1471-2105-12-150>

373

374 Robinson, J.W., Leshchyns'ka, I., Farghaian, H., Hughes, W.E., Sytnyk, V., Neely, G.G.,
375 Cole, A.R., 2014. PI4KII α phosphorylation by GSK3 directs vesicular trafficking to
376 lysosomes. *Biochem. J* 464, 145–156. <https://doi.org/10.1042/BJ20140497>

377

378 Strack, B., Calistri, A., Accola, M.A., Palu, G., Gottlinger, H.G., 2000. A role for
379 ubiquitin ligase recruitment in retrovirus release. *Proc. Natl. Acad. Sci. U. S. A.* 97,
380 13063–13068. <https://doi.org/10.1073/pnas.97.24.13063>

381

382 Thevenet, P., Shen, Y., Maupetit, J., Guyon, F., Derreumaux, P., Tufféry, P., 2012. PEP-
383 FOLD: an updated de novo structure prediction server for both linear and disulfide
384 bonded cyclic peptides. *Nucleic Acids Res.* 40, W288–93.
385 <https://doi.org/10.1093/nar/gks419>

386

387 To, K.K.-W., Tsang, O.T.-Y., Leung, W.-S., Tam, A.R., Wu, T.-C., Lung, D.C., Yip,
388 C.C.-Y., Cai, J.-P., Chan, J.M.-C., Chik, T.S.-H., Lau, D.P.-L., Choi, C.Y.-C., Chen, L.-
389 L., Chan, W.-M., Chan, K.-H., Ip, J.D., Ng, A.C.-K., Poon, R.W.-S., Luo, C.-T., Cheng,
390 V.C.-C., Chan, J.F.-W., Hung, I.F.-N., Chen, Z., Chen, H., Yuen, K.-Y., 2020. Temporal
391 profiles of viral load in posterior oropharyngeal saliva samples and serum antibody
392 responses during infection by SARS-CoV-2: an observational cohort study. *Lancet Infect.*
393 *Dis.* [https://doi.org/10.1016/S1473-3099\(20\)30196-1](https://doi.org/10.1016/S1473-3099(20)30196-1)

394

395 Trott, O., Olson, A.J., 2010. AutoDock Vina: improving the speed and accuracy of
396 docking with a new scoring function, efficient optimization, and multithreading. *J.*
397 *Comput. Chem.* 31, 455–461. <https://doi.org/10.1002/jcc.21334>

398

399 Vaguine, A.A., Richelle, J., Wodak, S.J., 1999. SFCHECK: a unified set of procedures
400 for evaluating the quality of macromolecular structure-factor data and their agreement
401 with the atomic model. *Acta Crystallogr. D Biol. Crystallogr.* 55, 191–205.

402 <https://doi.org/10.1107/S0907444998006684>

403

404 Wang, G.-Z., Chen, L.-L., Zhang, H.-Y., 2007. Phase-dependent nucleotide substitution
405 in protein-coding sequences. *Biochem. Biophys. Res. Commun.* 355, 599–602.

406 <https://doi.org/10.1016/j.bbrc.2007.01.006>

407

408 Wang, D.S., Shaw, R., Winkelmann, J.C., Shaw, G., 1994. Binding of PH domains of
409 beta-adrenergic receptor kinase and beta-spectrin to WD40/beta-transducin repeat
410 containing regions of the beta-subunit of trimeric G-proteins. *Biochem. Biophys. Res.*

411 *Commun.* 203, 29–35. <https://doi.org/10.1006/bbrc.1994.2144>

412

413 Wirblich, C., Tan, G.S., Papaneri, A., Godlewski, P.J., Orenstein, J.M., Harty, R.N.,
414 Schnell, M.J., 2008. PPEY motif within the rabies virus (RV) matrix protein is essential
415 for efficient virion release and RV pathogenicity. *J. Virol.* 82, 9730–9738.

416 <https://doi.org/10.1128/JVI.00889-08>

417

418 Yang, N., Ma, P., Lang, J., Zhang, Y., Deng, J., Ju, X., Zhang, G., Jiang, C., 2012.
419 Phosphatidylinositol 4-kinase III β is required for severe acute respiratory syndrome
420 coronavirus spike-mediated cell entry. *J. Biol. Chem.* 287, 8457–8467.

421 <https://doi.org/10.1074/jbc.M111.312561>

422

423 Yang, W.C., Ching, K.A., Tsoukas, C.D., Berg, L.J., 2001. Tec kinase signaling in T
424 cells is regulated by phosphatidylinositol 3-kinase and the Tec pleckstrin homology
425 domain. *J. Immunol.* 166, 387–395. <https://doi.org/10.4049/jimmunol.166.1.387>

426

427 Zaidman, D., Wolfson, H.J., 2016. PinaColada: peptide–inhibitor ant colony ad-hoc
428 design algorithm. *Bioinformatics* 32, 2289–2296.

429 <https://doi.org/10.1093/bioinformatics/btw133>

430

431 Zhang, T., Wu, Q., Zhang, Z., 2020. Probable Pangolin Origin of SARS-CoV-2
432 Associated with the COVID-19 Outbreak. *Curr. Biol.* 30, 1346–1351.e2.

433 <https://doi.org/10.1016/j.cub.2020.03.022>

434

435

436 **FIGURES LEGEND**

437

438 **Figure 1.** Multiple alignment of spike (S) protein of betacoronaviruses using the T-coffee
439 software. (A) Localization of PPxY Late domain in N-terminal. PPxY Late domain motifs
440 are colored in blue. The ²⁸YTNSF³² motif is indicated by green arrows. When its Tyr is
441 phosphorylated, it is able to bind Src Homology 2 (SH2) domain. GenBank and UniProt
442 accession numbers are indicated at the start of each sequence. The figure was prepared
443 using ESPript (<http://esprict.ibcp.fr>). (B) Alignment of codons of PPxY motifs. If
444 nucleotides in red in codons could mutate into cytosine, they would produce proline
445 residue. (C) Unrooted phylogenetic tree of S protein sequences of representative
446 betacoronaviruses. The tree was constructed using Mr Bayes method based on the multiple
447 alignment of complete S protein sequences by T-coffee. Betacoronaviruses in blue possess
448 a PPxY motif. GenBank and UniProt accession numbers are showed at the start of each
449 sequence.

450

451 **Figure 2.** Cartoon and surface representation of human Nedd4 WW3-domain (PDBid:
452 2KQ0_A) with docked peptides. (A) ²³QLPPAYTNS³¹ peptide of SARS-CoV-2 S protein
453 (cyan) and (B) ²³QLPPAYTNS³¹ superposed to Zaire Ebola virus Matrix protein VP40
454 (¹¹²TAPPEYMEA¹²⁰) peptide (green, PDBid: 2KQ0_B). (C) Surface representation of
455 Nedd4 WW3-domain with peptides depicted as sticks. Images were generated using PyMol
456 (www.pymol.org).

457

458

459

460

461

462

463

464

465

466

467 **Table 1. PPxY late-domain motif in single stranded enveloped RNA viruses.**

Viruses	Family	disease in human	Geography	PPxY protein	Reference
HIV-1	Retroviruses	AIDS	World	Gag	Strack et al., 2000
HTLV-1	Retroviruses	Aggressive lymphoma	World	Gag	Bouamr et al., 2003
Rhabies	Rhabdoviruses	Deadly brain inflammation	World	M	Harty et al., 2001
Marburg	Filoviruses	Deadly hemorrhagic fever	West Africa	VP40	Dolnik et al., 2010
Ebola	Filoviruses	Deadly hemorrhagic fever	West Africa	VP40	Harty et al., 2000
Lassa virus	Arenaviruses	Deadly hemorrhagic fever	West Africa	Z matrix	Baillet et al., 2019

468

469 **Table 2. ELM motifs of hot disordered loop in SARS-CoV-2 S protein.**

Elm Name	Instances	Positions	Elm Description	Cell compartment	Pattern
LIG_WW_1	PPAY	25-28	PPXY is the motif recognized by WW domains of Group I.	cytosol, membrane	PP.Y
LIG_SH2_STAP1	YTNSF	28-32	STAP1 Src Homology 2 (SH2) domain Class 2 binding motif.	plasma membrane	(Y)[DESTA][^GP][^GP][ILVF MWYA]
LIG_SH2_STAT5	YTNS	28-31	STAT5 Src Homology 2 (SH2) domain binding motif.	cytosol	(Y)[VLTFC]..
MOD_GSK3_1	PAYTNSFT	26-33	GSK3 phosphorylation recognition site.	cytosol, nucleus	...([ST])...[ST]
MOD_PIKK_1	TTRTQLP	19-25	(ST)Q motif which is phosphorylated by PIKK family members.	nucleus, cytosol	...([ST])Q..

470

471

A

	1	10	20	30	40																																											
YP_009724390.1_Human_SARS-CoV-2_China	M	F	V	F	L	V	L	L	P	E	V	S	S	Q	C	V	N	L	T	T	R	T	Q	L	P	F	A	V	T	.	.	N	S	F	T	R	G	V	Y	P	D	K	V	F	R	S		
P59594.1_Human_SARS-Cov_HongKong	M	F	T	F	L	L	F	.	L	T	T	S	G	S	D	L	D	R	C	T	T	F	D	D	V	Q	A	P	N	Y	T	Q	H	T	S	S	M	R	G	V	Y	P	D	E	I	F	R	S
QHR63300.2_Bat_coronavirus_RaTG13_China	M	F	V	F	L	V	L	.	L	P	E	V	S	S	Q	C	V	N	L	T	T	R	T	Q	L	P	F	A	V	T	.	.	N	S	T	R	C	V	Y	P	D	K	V	F	R	S		
QIA48623.1_Pangolin_PCoV_GX-P5L_China	M	F	V	F	L	F	V	.	L	P	E	V	S	S	Q	C	V	N	L	T	T	R	T	G	I	P	F	G	T	.	.	N	S	T	R	G	V	Y	P	D	K	V	F	R	S			
QIA48623.1_Pangolin_PCoV_GX-P1E_China	M	F	V	F	L	F	V	.	L	P	E	V	S	S	Q	C	V	N	L	T	T	R	T	G	I	Q	P	G	Y	T	.	.	N	S	T	R	G	V	Y	P	D	K	V	F	R	S		
AVP78031.1>_Bat_CoVZC45_CoV_China	M	L	F	F	L	F	L	Q	F	A	L	V	N	S	Q	C	V	N	L	T	G	R	T	P	L	N	P	N	Y	T	.	.	N	S	S	Q	R	G	V	Y	P	D	T	I	Y	R	S	
ATO98205.1>_Bat_Rs4874_CoV_China	M	F	T	F	L	F	F	.	L	T	T	S	G	S	D	L	E	S	C	T	T	F	D	D	V	Q	A	P	N	Y	T	Q	H	T	S	S	R	G	V	Y	P	D	E	I	F	R	S	

▲▲ ▲▲▲

472

B

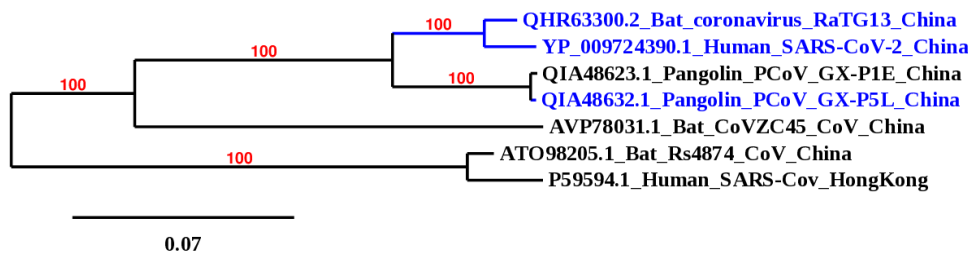
SARS-CoV-2	ccc cct gca tac
SARS-CoV	ctt cct aat tac
Bat_coronavirus_RaTG13	cct cct gca tac
Pangolin_PCoV_GX-P5L	ccg cca ggt tat
Pangolin_PCoV_GX-P1E	cag cca ggt tat
Bat_CoVZC45_CoV	aat ccc aat tat
Bat_Rs4874_CoV	cc cct aat tac

473

474

475

C



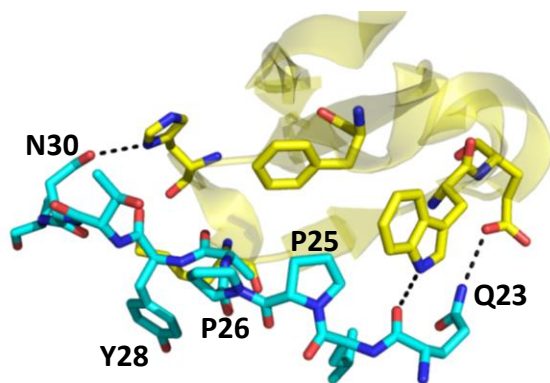
476

477

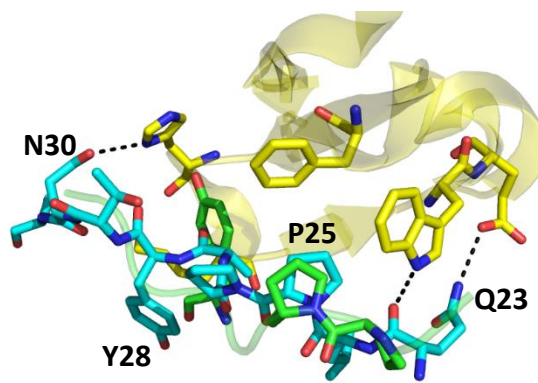
Fig. 1

478

A



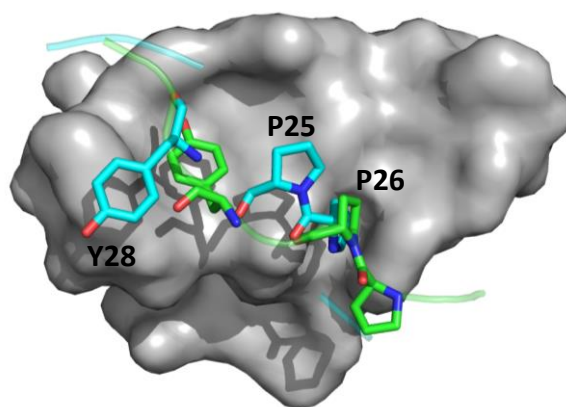
B



479

480

C



481

482 **Fig. 2**